

## Stability of Branched Tubular Membrane Structures

Maike Jung,<sup>1,\*</sup> Gerhard Jung<sup>2</sup>, and Friederike Schmid<sup>1,†</sup>

<sup>1</sup>*Institut für Physik, Johannes Gutenberg-Universität Mainz, Staudingerweg 9, 55128 Mainz, Germany*

<sup>2</sup>*Laboratoire Charles Coulomb (L2C), Université de Montpellier, CNRS, 34095 Montpellier, France*



(Received 27 May 2022; accepted 15 February 2023; published 6 April 2023)

We study the energetics and stability of branched tubular membrane structures by computer simulations of a triangulated network model. We find that triple (Y) junctions can be created and stabilized by applying mechanical forces, if the angle between branches is  $120^\circ$ . The same holds for tetrahedral junctions with tetrahedron angles. If the wrong angles are enforced, the branches coalesce to a linear structure, a pure tube. After releasing the mechanical force, Y-branched structures remain metastable if one constrains the enclosed volume and the average curvature (the area difference) to a fixed value; tetrahedral junctions however split up into two Y junctions. Somewhat counterintuitively, the energy cost of adding a Y branch is negative in structures with fixed surface area and tube diameter, even if one accounts for the positive contribution of the additional branch end. For fixed average curvature, however, adding a branch also enforces a thinning of tubes, therefore the overall curvature energy cost is positive. Possible implications for the stability of branched networks structures in cells are discussed.

DOI: [10.1103/PhysRevLett.130.148401](https://doi.org/10.1103/PhysRevLett.130.148401)

Tubular membrane network structures are abundant in biological cells, for example, in the Golgi complex [1,2] and the endoplasmic reticulum [3,4]. Such tubular networks are highly dynamic structures [5], in which new tubes are constantly created and existing tubes are merged or dissolved. Potential physiological roles of the three-dimensional tubular network spanning the endoplasmic reticulum include membrane trafficking, lipid metabolism, and autophagy, i.e., the cleaning mechanism of the cell [4]. The function of the tubular network in the Golgi apparatus appears to be the interconnection of different building blocks, which can also induce structural rearrangements during cell differentiation [6]. Membrane nanotubes have also been found to generally enhance intercellular transport [7]. Understanding the formation and stability of tubular networks is thus a critical problem in the fields of biology, biophysics and soft matter.

The formation of tubular structures and membrane networks can be induced by various different mechanisms, which can be classified into different categories [8]. The most obvious way of creating tubular structures is by a force acting on a localized point on the membrane surface. This force can be induced by growing filaments (filament bundles) which are attached to the membrane [9,10] or by a concerted action of molecular motors [11–16]. Other mechanisms for tube formation include scaffolding, in which proteins are polymerizing on the surface of the membrane, effectively forcing the membrane to adopt the shape of the proteins [17,18], and the adsorption or inclusion of curvature-inducing proteins, which have been widely observed in nature [19,20] and can induce either positive or negative curvature [21,22]. For example,

reticulin has been found to induce the tubular network structure in the endoplasmic reticulum [23–25].

From a theoretical point of view, membrane shapes have been studied intensely for many decades [26–28], often using elastic continuum models based on the Canham-Helfrich theory [29–31]. Already for structures with simple sphere topology, the shape diagrams were found to be surprisingly complex, with first and second order transitions between prolate, oblate, pear, and stomatocyte shapes [26,32–34]. The process of mechanically pulling tubes from vesicles has been investigated in detail by experiment, theory, and simulation [35–42] and found to be accompanied by a free energy barrier [39], suggesting that it might be possible to create metastable tubular structures using mechanical forces (e.g., molecular motors). Indeed, Bahrami *et al.* [43] have recently demonstrated by computer simulations that linear tubular structures can be metastable even in the absence of forces and curvature-inducing proteins, as long as the enclosed volume is kept fixed. This is due to the existence of a free energy barrier between the linear tube shape and the true minimum-energy shapes, which are oblate and prolate structures for thick tubes and stomatocytes in the case of thin tubes.

While the (meta)stability of linear tubular structures has been analyzed in some detail, a network has a second fundamental building block, i.e., the junctions where several tubes merge. Detailed theoretical analyses of such branched structures, comparable to the ones for cylindrical tubes, however, are still missing. In the present Letter, we aim to fill this gap. We will first consider force-stabilized branched structures and examine their stability. Then we will establish conditions under which force-free branched structures can be metastable.

*Model and method.*—Our starting point is the simplest continuum description of two-dimensional fluid membranes on large scales, the so-called Helfrich Hamiltonian [29–31],

$$H_{cv} = \frac{\kappa}{2} \int dA K^2 + \bar{\kappa} \int dA K_G. \quad (1)$$

Here  $\kappa$ ,  $\bar{\kappa}$  are curvature moduli (for lipid membranes,  $\kappa$  is typically of order  $20k_B T$  [44]),  $K$  is the total curvature, and  $K_G$  the Gaussian curvature. We consider closed structures with fixed sphere topology, hence the last term is a constant according to the Gauss-Bonnet theorem [45] and can be omitted. We note that we have not included a spontaneous curvature term in Eq. (1). Instead, we will discuss the effect of imposing an integrated average curvature  $\int dA K$  in the spirit of the area difference elasticity (ADE) model [46–49]. The physical origin of this global curvature could be asymmetric numbers of lipid in the inner and outer membrane leaflet (“area difference”) [31,46–52].

The theory is solved numerically using a dynamically triangulated surface model [43,53–64]. Specifically, we use the version of Noguchi and Gompper [65] which is described in detail in Ref. [66]. The surface is described by a network of  $N$  vertices that are connected by bonds in a triangular network structure [ $N_\Delta = 2(N - 2)$  triangles], and the simulation is a combination of Brownian dynamics (node motion) and Monte Carlo moves (bond flips). We fix the area ( $A = A_0$ ) and in some simulations also the enclosed volume  $V$  and the dimensionless average curvature (the area difference) [43,46–49]  $\Delta a = (1/4\sqrt{\pi A_0}) \int dA K$  by introducing harmonic constraint potentials with spring constants  $k_A$ ,  $k_V$ , and  $k_{\Delta a}$ . Details of the implementation can be found in Supplemental Material [67].

In the following, results are given in units of  $l_b$  (typical bond length),  $\epsilon = (\kappa/20)$  (energy unit), and  $\tau = l_b \sqrt{m\epsilon}^{-1}$  (time unit), where  $m$  is the mass of the vertices. Unless stated otherwise, the remaining parameters are  $k_B T = 1\epsilon$ ,  $N = 2562$ ,  $A_0 = 0.41 l_b^2 \cdot N_\Delta$ ,  $k_A = 2\epsilon/l_b^2$ ,  $k_V = k_{\Delta a} = 0$ , and the simulation time step is  $\Delta t = 10^{-4}\tau$ . Constraints on  $V$  and/or  $\Delta a$  are imposed by setting  $k_V = 1\epsilon/l_b^3$  and/or  $k_{\Delta a} = 1\epsilon$ . The enclosed volume will be characterized by the dimensionless quantity  $\nu = 6\sqrt{\pi/A^3}V$ . The reference values of  $\nu$  and  $\Delta a$  for perfect spheres are thus  $\nu = \Delta a = 1$ .

*Force-stabilized linear and branched tubular structures.*—To create tubular structures, forces with amplitude  $F_{\text{ext}}$  are applied to a set of  $n$  vertices such that the total force is zero ( $n = 2, 3, 4$ ). For  $n = 2$ , linear tubes are obtained. For  $n = 3$ , a branched structure with a Y junction can be stabilized, provided the forces lie in one plane and have an angle of  $120^\circ$  to each other [see Fig. 1(a)], otherwise one creates linear structures as well. Using  $n = 4$ , one can create mechanically forced tetrahedral junctions; all other fourfold junctions are unstable and separate into Y junctions (see Supplemental Material [67], Fig. 1

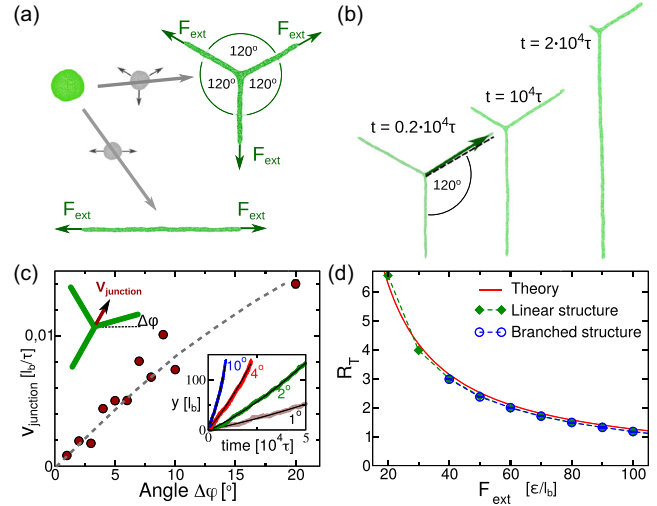


FIG. 1. Force-stabilized tubular structures. (a) Illustration of creation process. The starting point is a force-free spherical vesicle. To create linear structures, two opposing forces are applied at opposing vertices while keeping the area  $A$  fixed (no other constraints). Y-branched structures are obtained by applying three coplanar forces with angles  $120^\circ$  to each other. (b) Evolution of a Y-branched structure with time  $t$  at  $F_{\text{ext}} = 90\epsilon/l_b$  if the direction of one applied force deviates from the symmetric direction by  $\Delta\varphi = 4^\circ$  [69]. (c) Initial velocity of the junction as a function of  $\Delta\varphi$  at  $F_{\text{ext}} = 90\epsilon/l_b$ . The dashed line is a guide for the eye. Inset shows the displacement  $y$  of the junction from its initial position versus time for different  $\Delta\varphi$  as indicated, along with a quadratic fit to  $y = y_0 + v_{\text{junction}}t + bt^2$  (black lines). (d) Tube radius versus applied force  $F_{\text{ext}}$  for linear (green diamond) and branched structures (blue circles), compared with theory (red line).

and movies `4fold.mp4`, `4fold_twisted.mp4`, `tetrahedral.mp4`).

Y junctions with fixed angle  $120^\circ$  are characteristic of the so-called Fermat point, the state that minimizes the total tube length of a network if the tube ends are kept at fixed positions. In experimental studies, artificial surfactant and liposome networks with fixed tube ends were found to always evolve towards the Fermat point [70–72]. Our simulations show that these  $120^\circ$  Y junctions remain the only stable triple junctions even in situations where the tube ends are mobile. Figure 1(b) shows the effect of slightly perturbing the angle of one applied force from  $120^\circ$ , starting from the configuration Fig. 1(a): The junction starts moving in the direction of the smallest angle until it disappears, with a velocity that is roughly proportional to the distortion  $\Delta\varphi$  [Fig. 1(c)].

For stable branched structures, the presence of the junction has little effect on the structure of the connected tubes. The tube radius  $R_T$  as a function of the applied force  $F_{\text{ext}}$  is the same for linear and branched structures and consistent with the theoretical estimate [11,35]  $R_T = 2\pi\kappa/F_{\text{ext}}$  [Fig. 1(d)].

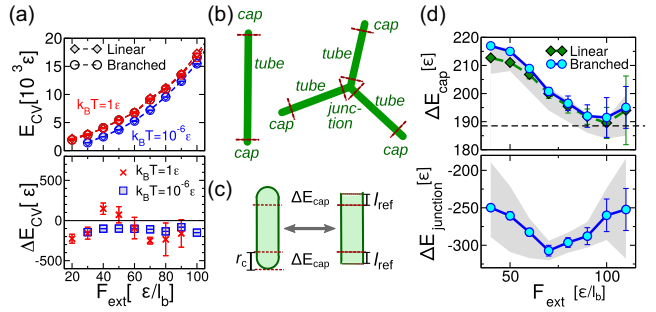


FIG. 2. Curvature energies of force-stabilized tubular structures. (a) Top: Elastic energy for linear (diamonds) and branched (circles) structures as a function of applied force  $F_{\text{ext}}$  at  $k_B T = 1\epsilon$  (red) and  $k_B T = 10^{-6}\epsilon$  (blue). Bottom: Difference between the curvature energy of branched and linear structures  $k_B T = 1\epsilon$  (red crosses) and  $k_B T = 10^{-6}\epsilon$  (blue squares). (b) Cartoon showing dissection of structures into tubes, caps and junctions (see text). (c) Cartoon illustrating the definition of excess energies: The energy of a tubular structure is compared to that of a reference tubular section with the same area. (d) Excess curvature energy of caps (top) and junctions (bottom) for linear (green diamonds) and branched (blue circles) structures, obtained at  $k_B T = 10^{-6}\epsilon$ . Dashed line (top) shows theoretical value for ideal semispherical caps. Symbols or lines show values obtained with cutoff parameters  $r_{c,\text{cap}} = 8l_b$  and  $r_{c,\text{junction}} = 20l_b$ . Gray shaded areas indicate spread of results if one varies the cutoff between  $r_{c,\text{cap}} \in [7, 10]l_b$  and  $r_{c,\text{junction}} \in [10, 25]l_b$ .

Next we analyze the curvature energy (1) of the different structures. Figure 2(a) shows the results at temperature  $k_B T = 1$  and after annealing to  $k_B T = 10^{-6}\epsilon \approx 0$  for linear and branched structures. The energies at  $k_B T = 1\epsilon$  and  $k_B T \approx 0$  differ by roughly  $N/2$ , indicating that this energy difference can be attributed to thermal out-of-plane fluctuations of vertices. Interestingly, the elastic energy of branched structures is found to be *lower* than that of linear structures [Fig. 2(a), lower panel].

To analyze this in more detail, we calculate separately the excess elastic energy of caps (tube ends) and junctions relative to a reference cylindrical tube section with the same radius and the same area [see Fig. 2(c)]: We separate the structures into “caps,” “junctions,” and “tubular” sections as indicated in Fig. 2(b), extract an elastic energy  $e$  per tube length from the tubular sections, and evaluate the excess energies of caps and junctions via  $\Delta E_{\text{cap,junction}} = E_{\text{cap,junction}} - l_{\text{ref}}e$ , where  $l_{\text{ref}} = A_{\text{cap,junction}}/2\pi R_T$  is the length of the reference tube section. For example, the ideal values for semispherical caps are  $e = \pi\kappa/R_T$  and  $\Delta E_{\text{cap}} = 3\pi\kappa$ , and this is independent of the cutoff value  $r_c$  marking the end of the cap region as long as  $r_c > R_T$ . The procedure thus largely removes the dependence of the results on the specific dissection into junctions, caps, and tubular regions.

In practice, the results are still somewhat sensitive to the choice of the cutoff values  $r_c$  [Fig. 2(d), shaded areas]. Even taking these uncertainties into account, it is clear that

the excess energy of caps is positive ( $\Delta E_{\text{cap}} = 190\text{--}220\epsilon$  depending on the applied force) and the excess energy of junctions is negative ( $\Delta E_{\text{junction}} \approx -280\epsilon$ ). The excess energy of caps is higher than the theoretical estimate  $E_{\text{cap}} = 3\pi\kappa$ , which we attribute to some extra distortion in the vicinity of the vertex where the force  $F_{\text{ext}}$  is applied. The negative excess energy of junctions reflects the fact that the overall curvature in the region of the junction is reduced. Interestingly, in branched structures, the energy gain at junctions more than compensates the energy loss due to the formation of an additional cap. As a result, the total elastic energy of branched structures is lower than that of linear structures.

*Force-free (meta)stable structures.*—We turn to the question whether branched structures can be metastable in the absence of forcing. Bahrami *et al.* [43] have recently observed that linear structures remain metastable if the enclosed volume  $V_0$  is fixed. Motivated by their findings, we study in Fig. 3(a) the time evolution of linear and branched structures after releasing a stabilizing force while keeping  $V_0$  fixed. In both cases, the structures eventually transform into a structure with lower energy, a stomatocyte [see Fig. 3(c)]. However, the transformation process is qualitatively different. In branched structures, it sets in immediately via a disclike widening at the junction (see Supplemental Material movie `branch_fixNu.mp4`). Linear structures initially remain (meta)stable for some

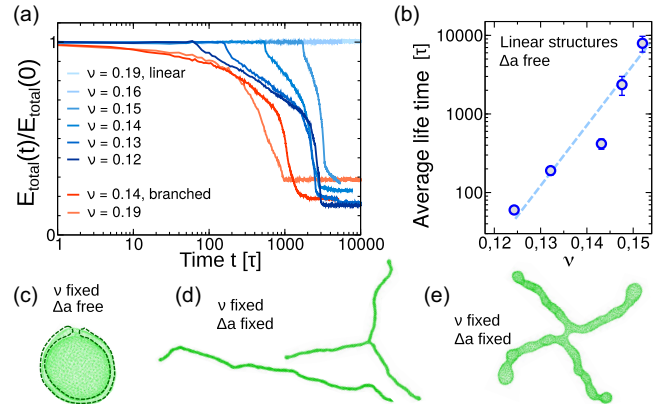


FIG. 3. Stability of force-free tubular structures. (a) Examples of time evolution of the total energy after releasing the force on force-stabilized linear (blue) and branched (red) structures at fixed  $\nu$  as indicated ( $\Delta a$  is not constrained). Both structures eventually transform into a stomatocyte. For linear structures, the transformation process sets in after an activation time, which exceeds the maximum simulation time for  $\nu > 0.15$ . (b) Average lifetime of linear structures after releasing the stabilizing force as a function of  $\nu$  ( $\Delta a$  is free). Dashed line shows exponential behavior. (c) Example of a stable stomatocyte structure with  $\nu = 0.14$ . (d) Stable linear and branched structure if both  $\nu$  and  $\Delta a$  are fixed ( $\nu = 0.14$ ). (e) Structure obtained after releasing the force from a force-stabilized tetrahedral structure at fixed  $\nu$  and  $\Delta a$  (at  $\nu = 0.2$ ). The tetrajunction splits up into two Y junctions.

activation time, indicating that the shape change is an activated process. The transformation is then initiated by the nucleation of a disc at one end (see Supplemental Material movie `linear_fixNu.mp4` [67]). The activation time of linear structures increases roughly exponentially with  $\nu$  [see Fig. 3(b)] and eventually exceeds the total simulation time, consistent with [43].

Imposing a small reduced volume alone is thus not sufficient to stabilize branched structures. However, constraining the average curvature  $\Delta a$  in addition to  $\nu$  does have a stabilizing effect. Supplemental Material Figs. 2(a) and 2(b) [67] show that  $\Delta a$  drops substantially during the transformation from tubular or branched structures to stomatocyte. If one constrains  $\Delta a$  to its initial value, i.e., the value of the force-stabilized structure, this suppresses the transformation, and the tubular or branched structures with Y junctions remain (meta)stable. Examples are shown in Fig. 3(d). Tetrahedral junctions, on the other hand, do not persist, but separate into two Y junctions [see Fig. 3(d), Supplemental Material Fig. 2(e) and Supplemental Material movie `f0_tetrahedral_nu20fixDa.mp4` [67]]. If only  $\Delta a$  is kept fixed, linear and branched structures are also stable, but may acquire slightly pearled shapes, see Supplemental Material Fig. 2(d) [67].

*Origin of energy penalty for junction defects.*—The question remains which of the two structures, branched, or linear, has the lower energy. Judging from our previous results on excess cap and junction energies (Fig. 2), one might suspect that branching is energetically favorable. However, the situation is more subtle. Adding a junction locally removes curvature in the junction region, which has to be added elsewhere to keep  $\Delta a$  fixed. As a result, the tubular sections become thinner, and their curvature energy increases. In Supplemental Material [67], we present a theoretical estimate showing that the resulting net energy difference is roughly given by  $E_{CV,branch} - E_{CV,linear} \sim \pi\kappa + |\epsilon \cdot \Delta E_{CV,junction}| > 0$ , where  $\epsilon$  characterizes the reduction of curvature at the junction. At fixed  $\Delta a$ , the total curvature energy of branched structures should hence be higher than that of linear structures. A similar effect is expected for fixed  $\nu$ : A junction adds enclosed volume, which has to be removed elsewhere, leading again to a thinning of tubes.

The net effect of constraints on the curvature energy as obtained from simulations is summarized in Table I for the example of force-stabilized structures at  $F_{ext} = 70\epsilon/l_b$ . Here, we have used the values of  $\nu$  and/or  $\Delta a$  obtained for unconstrained force-stabilized linear structures (parameter set C1) and branched structures (parameter set C2) as input parameters in constrained force-stabilized simulations of linear and branched structures. The curvature energies obtained with the set C1 are generally higher than those obtained with C2, because  $\Delta a$  is higher and/or  $\nu$  is lower. Comparing linear and branched structures for the same parameter set, the results confirm the expectations of the discussion above. Only in the absence of any constraints is

TABLE I. Curvature energies  $E_{CV}$ , reduced volumes  $\nu$ , and average curvatures  $\Delta a$  for force-stabilized pure linear and branched structures at  $F_{ext} = 70\epsilon/l_b$ . Results are shown for two sets of constraints C1 and C2 on  $\nu$ ,  $\Delta a$ , or both as indicated, which correspond to the values obtained for unconstrained force-stabilized linear and branched structures, respectively.

Fixed	Structure	$E_{CV}/\epsilon$		$\nu$		$\Delta a$	
	Linear	$9333 \pm 26$		$0.186 \pm 0.001$		$3.90 \pm 0.01$	
	Branched	$9082 \pm 34$		$0.193 \pm 0.001$		$3.81 \pm 0.01$	
		C1 (Linear)			C2 (Branched)		
		$E_{CV}$	$\nu$	$\Delta a$	$E_{CV}$	$\nu$	$\Delta a$
$\Delta a$	Linear	$9333 \pm 3$	0.186	3.90	$8975 \pm 3$	0.191	3.81
	Branched	$9470 \pm 3$	0.187	3.90	$9117 \pm 3$	0.192	3.81
$\nu$	Linear	$9355 \pm 3$	0.186	3.91	$8882 \pm 3$	0.192	3.79
	Branch	$9538 \pm 4$	0.186	3.92	$9079 \pm 4$	0.193	3.80
$\nu, \Delta a$	Linear	$9342 \pm 3$	0.186	3.90	$8951 \pm 3$	0.192	3.81
	Branch	$9480 \pm 3$	0.186	3.90	$9126 \pm 3$	0.193	3.81

the curvature energy of branched structures lower than that of linear structures. In all other cases (constraints on  $\nu$ , on  $\Delta a$ , on both), the curvature energy of branched structures is higher.

*Conclusions.*—To summarize, we have investigated the energetics and stability of an essential component of tubular membrane networks, the junctions, from the point of view of the Canham-Helfrich elastic theory of membranes. We consider membrane structures with closed sphere topology and allow for constraints on the enclosed volume  $\nu$  and the average curvature  $\Delta a$ , without, however, imposing specific local curvatures. Within this simple model, we find that Y junctions with angles  $120^\circ$  can be stabilized by mechanical forces and remain metastable after releasing the forces. Other types of junctions and other angles are unstable. Furthermore, we find that Y junctions locally have a negative excess curvature energy. For fixed tube diameter, branching is energetically favorable, even if one accounts for the positive energy of the additional cap. At fixed  $\Delta a$ , however, adding a branch enforces a thinning of the tubes, such that the overall curvature energy balance disfavors branching.

This subtle energy balance should lead to an increase of the lifetime of metastable branches, as their elimination is only favorable if the entire tube network rearranges. In addition, dynamical simulations suggest that the creation and annihilation of branches is accompanied by a free energy barrier: Pulling a branch out of a tube requires slightly higher forces than needed to stabilize it [see Supplemental Material, Fig. 2(a)] and if one annihilates a branch by pulling on the other tubes, the curvature energy passes through a maximum [Supplemental Material, Fig. 2(b)].

Our results thus indicate that simple properties of elastic membranes might be responsible for the abundance of tube

network structures in cells. These structures are already metastable and long lived if one imposes a few generic constraints, such as a fixed surface area difference between inner and outer membrane leaflet and possibly impermeability (fixed enclosed volume; not strictly necessary). Hence they can be stabilized and manipulated with little extra effort.

We have studied a very idealized model of bare membranes. However, given the generic character of our main conclusions, we expect them to still hold in other membrane models, e.g., ADE models with more realistic (lower) area difference elasticities  $k_{\Delta a}$ , or membrane structures with average curvature imposed by freely moving curvature-inducing proteins [19–24], where one has to account for their entropy of mixing. This will be an interesting subject for future studies.

We thank Enrico Schleiff for motivating this project, Hiroshi Noguchi from the ISSP at the University of Tokyo, Japan, for helpful discussions and for sharing the source code of his dynamically triangulated membrane model [66], which was extended by us to include area difference constraints. The simulations were carried out on the supercomputer Mogon at Johannes Gutenberg University Mainz. This work was funded by the state of Rhineland-Palatinate, Germany, within the Dynamem consortium, and in part by the Deutsche Forschungsgemeinschaft (DFG, German Research Foundation)—Project No. 233630050—TRR 146.

\*maike\_lauf@web.de

†friederike.schmid@uni-mainz.de

- [1] H. Mollenhauer and D. Morre, *Histochem. Cell Biol.* **109**, 533 (1998).
- [2] M. De Matteis and A. Luini, *Nat. Rev. Mol. Cell Biol.* **9**, 273 (2008).
- [3] L. Westrate, J. Lee, W. Prinz, and G. Voeltz, *Annu. Rev. Biochem.* **84**, 791 (2015).
- [4] L. Lü, L. Niu, and J. Hu, *Biophys. Rep.* **6**, 105 (2020)
- [5] R. E. Powers, S. Wang, T. Y. Liu, and T. A. Rapoport, *Nature (London)* **543**, 257 (2017).
- [6] J. Saraste and K. Prydz, *Front. Cell Dev. Biol.* **7**, 171 (2019).
- [7] S. Sowinski, C. Jolly, O. Berninghausen, M. Purbhoo, A. Chauveau, K. Köhler, S. Oddos, P. Eissmann, F. Brodsky, C. Hopkins, B. Önfelt, Q. Sattentau, and D. Davis, *Nat. Cell Biol.* **10**, 211 (2008).
- [8] A. Roux, *Soft Matter* **9**, 6726 (2013).
- [9] H. Miyata and H. Hotani, *Proc. Natl. Acad. Sci. U.S.A.* **89**, 11547 (1992).
- [10] H. Miyata, S. Nishiyama, K.-i. Akashi, and K. Kinoshita, *Proc. Natl. Acad. Sci. U.S.A.* **96**, 2048 (1999).
- [11] I. Derényi, F. Jülicher, and J. Prost, *Phys. Rev. Lett.* **88**, 238101 (2002).
- [12] G. Koster, M. VanDuijn, B. Hofs, and M. Dogterom, *Proc. Natl. Acad. Sci. U.S.A.* **100**, 15583 (2003).
- [13] C. Leduc, O. Campàs, K. B. Zeldovich, A. Roux, P. Jolimaître, L. Bourel-Bonnet, B. Goud, J.-F. Joanny, P. Bassereau, and J. Prost, *Proc. Natl. Acad. Sci. U.S.A.* **101**, 17096 (2004).
- [14] O. Campàs, C. Leduc, P. Bassereau, J. Casademunt, J.-F. Joanny, and J. Prost, *Biophys. J.* **94**, 5009 (2008).
- [15] R. Nambiar, M. R. E., and M. J. Tyska, *Proc. Natl. Acad. Sci. U.S.A.* **106**, 11972 (2009).
- [16] W. Du, Q. Su, Y. Chen, Y. Zhu, D. Jiang, Y. Rong, S. Zhang, Y. Zhang, H. Ren, C. Zhang, X. Wang, N. Gao, Y. Wang, L. Sun, Y. Sun, and L. Yu, *Dev. Cell* **37**, 326 (2016).
- [17] M. J. Footer, J. W. J. Kerssemakers, J. A. Theriot, and M. Dogterom, *Proc. Natl. Acad. Sci. U.S.A.* **104**, 2181 (2007).
- [18] A. Roux, G. Koster, M. Lenz, B. Sorre, J.-B. Manneville, P. Nassoy, and P. Bassereau, *Proc. Natl. Acad. Sci. U.S.A.* **107**, 4141 (2010).
- [19] I. Tsafrir, Y. Caspi, M.-A. Guedeau-Boudeville, T. Arzi, and J. Stavans, *Phys. Rev. Lett.* **91**, 138102 (2003).
- [20] Y. Shibata, J. Hu, M. M. Kozlov, and T. A. Rapoport, *Annu. Rev. Cell Dev. Biol.* **25**, 329 (2009).
- [21] F. Campelo, H. T. McMahon, and M. M. Kozlov, *Biophys. J.* **95**, 2325 (2008).
- [22] A. Frost, V. M. Unger, and P. De Camilli, *Cell* **137**, 191 (2009).
- [23] G. K. Voeltz, W. A. Prinz, Y. Shibata, J. M. Rist, and T. A. Rapoport, *Cell* **124**, 573 (2006).
- [24] J. Hu, Y. Shibata, C. Voss, T. Shemesh, Z. Li, M. Coughlin, M. M. Kozlov, T. A. Rapoport, and W. A. Prinz, *Science* **319**, 1247 (2008).
- [25] T. Shemesh, R. W. Klemm, F. B. Romano, S. Wang, J. Vaughan, X. Zhuang, H. Tukachinsky, M. M. Kozlov, and T. A. Rapoport, *Proc. Natl. Acad. Sci. U.S.A.* **111**, E5243 (2014).
- [26] U. Seifert and R. Lipowsky, *Struct. Dyn. Membr.* **1**, 403 (1995).
- [27] N. Ramakrishnan, R. P. Bradle, R. W. Tourdot, and R. Radhakrishnan, *J. Phys. Condens. Matter* **30**, 273001 (2018).
- [28] R. Lipowsky, *Adv. Biol.* **6**, 2101020 (2021).
- [29] P. Canham, *J. Theor. Biol.* **26**, 61 (1970).
- [30] W. Helfrich, *Z. Naturforsch.* **28C**, 693 (1973).
- [31] E. A. Evans, *Biophys. J.* **14**, 923 (1974).
- [32] U. Seifert, K. Berndl, and R. Lipowsky, *Phys. Rev. A* **44**, 1182 (1991).
- [33] G. Gompper and D. M. Kroll, *Phys. Rev. E* **51**, 514 (1995).
- [34] C. Vanhille-Campos and A. Saric, *Soft Matter* **17**, 3798 (2021).
- [35] L. Bo and R. Waugh, *Biophys. J.* **55**, 509 (1989).
- [36] D. J. Bukman, J. H. Yao, and M. Wortis, *Phys. Rev. E* **54**, 5463 (1996).
- [37] C. R. Calladine and J. A. Greenwood, *J. Biomech. Eng.* **124**, 576 (2002).
- [38] A.-S. Smith, E. Sackmann, and U. Seifert, *Phys. Rev. Lett.* **92**, 208101 (2004).
- [39] G. Koster, A. Cacciuto, I. Derényi, D. Frenkel, and M. Dogterom, *Phys. Rev. Lett.* **94**, 068101 (2005).
- [40] I. Golushko and S. Rochal, *J. Exp. Theor. Phys.* **122**, 169 (2016).
- [41] H. Noguchi, *Soft Matter* **17**, 10469 (2021).
- [42] A. Paraschif, T. J. Lagny, C. Vanhille-Campos, E. Coudrier, P. Bassereau, and A. Saric, *Biophys. J.* **120**, 598 (2021).

- [43] A. H. Bahrami and G. Hummer, *ACS Nano* **11**, 9558 (2017).
- [44] W. Rawicz, K. Olbrich, T. McIntosh, D. Needham, and E. Evans, *Biophys. J.* **79**, 328 (2000).
- [45] M. D. Carmo, *Differential Geometry of Curves and Surfaces* (Prentice Hall, Englewood Cliffs, NJ, 1976).
- [46] B. Bozic, S. Svetina, B. Zeks, and R. Waugh, *Biophys. J.* **61**, 963 (1992).
- [47] W. Wiese, W. Harbich, and W. Helfrich, *J. Phys. Condens. Matter* **4**, 1647 (1992).
- [48] V. Heinrich, S. Svetina, and B. Žekš, *Phys. Rev. E* **48**, 3112 (1993).
- [49] L. Miao, U. Seifert, M. Wortis, and H.-G. Döbereiner, *Phys. Rev. E* **49**, 5389 (1994).
- [50] M. Sheetz and S. Singer, *Proc. Natl. Acad. Sci. U.S.A.* **71**, 4457 (1974).
- [51] S. Svetina and B. Zeks, *Eur. Biophys. J.* **17**, 101 (1989).
- [52] P. Zihler and S. Svetina, *Europhys. Lett.* **70**, 690 (2005).
- [53] Itzykson, *Proceedings of the GIFT Seminar, Jaca85* (World Scientific, Singapore, 1986).
- [54] Y. Kantor and D. R. Nelson, *Phys. Rev. Lett.* **58**, 2774 (1987).
- [55] G. Gompper and D. M. Kroll, *J. Phys. I France* **6**, 1305 (1996).
- [56] G. Gompper and D. M. Kroll, *J. Phys. Condens. Matter* **9**, 8795 (1997).
- [57] F. Jülicher, *J. Phys. II* **6**, 1797 (1996).
- [58] A. Šarić and A. Cacciuto, *Phys. Rev. Lett.* **109**, 188101 (2012).
- [59] A. H. Bahrami, R. Lipowsky, and T. R. Weikl, *Phys. Rev. Lett.* **109**, 188102 (2012).
- [60] N. Ramakrishnan, P. Sunil Kumar, and J. H. Ipsen, *Biophys. J.* **104**, 1018 (2013).
- [61] A. Vahid, A. Šarić, and T. Idema, *Soft Matter* **13**, 4924 (2017).
- [62] B. Li and S. M. Abel, *Soft Matter* **14**, 185 (2018).
- [63] M. Hoore, F. Yaya, T. Podgorski, C. Wagner, G. Gompper, and D. A. Fedosov, *Soft Matter* **14**, 6278 (2018).
- [64] X. Bian, S. Litvinov, and P. Koumoutsakos, *Comput. Methods Appl. Mech. Eng.* **359**, 112758 (2020).
- [65] H. Noguchi and G. Gompper, *Phys. Rev. Lett.* **93**, 258102 (2004).
- [66] H. Noguchi and G. Gompper, *Phys. Rev. E* **72**, 011901 (2005).
- [67] See Supplemental Material at <http://link.aps.org/supplemental/10.1103/PhysRevLett.130.148401> for a detailed description of the model, snapshots, and movies on transformation pathways, additional calculations, and additional Ref. [68].
- [68] F. H. Stillinger and T. A. Weber, *Phys. Rev. B* **31**, 5262 (1985).
- [69] A small compensating force is applied to all  $N$  vertices to ensure that the total force is still zero.
- [70] T. Lobovkina, P. Dommersnes, J.-F. Joanny, P. Bassereau, M. Karlsson, and O. Orwar, *Proc. Natl. Acad. Sci. U.S.A.* **101**, 7949 (2004).
- [71] T. Lobovkina, P. Dommersnes, J.-F. Joanny, J. Hurtig, and O. Orwar, *Phys. Rev. Lett.* **97**, 188105 (2006).
- [72] T. Lobovkina, P. Dommersnes, S. Tiourine, J.-F. Joanny, and O. Orwar, *Eur. Phys. J. E* **26**, 295 (2008).